Metal-Insulator-Semiconductor Transmission Line Model

Dylan F. Williams, *Senior Member, IEEE*
National Institute of Standards and Technology
325 Broadway, Boulder, CO 80303
Ph: (303)497-3138 Fax: (303)497-3122 E-mail: dylan@boulder.nist.gov

Abstract- **This paper investigates the one-dimensional metal-insulator-semiconductor transmission line. It develops closed-form expressions for equivalent-circuit parameters, compares them to exact calculations, and explores their limitations. It also investigates the usual assumption of single-mode propagation and shows that, in certain fairly common circumstances, the fundamental mode of propagation becomes so lossy that it can no longer be considered to be the dominant propagating mode.**

INTRODUCTION

This paper investigates the transverse-magnetic (TM) modes of the one-dimensional metal-insulator-semiconductor (MIS) transmission line of Fig. 1. The transmission line consists of a metal film bounded on its upper surface by a perfect magnetic wall and separated by an insulator or a depletion region from a semiconducting substrate backed with a perfectly conducting wall. While this transmission line has no fringing fields, it approximates wide microstrip lines fabricated on silicon substrates. Its solutions, when reflected through the magnetic wall, also correspond to those of the even modes of symmetric infinitely wide metal-semiconductor-insulator-metal-insulator-semiconductor-metal striplines.

Guckel et al. [1], Hasegawa et al. [2], and Jäger [3] first investigated the one-dimensional MIS transmission line. Guckel et al. observed that, when the substrate conductivity σ_s is greater than a specific conductivity σ_{min}, the MIS line will be dominated by series loss, and that, when σ_s is less than σ_{min}, the MIS line will be dominated by shunt loss. They used σ_{min} to define two distinct regions of operation. They treated these two regions of operation independently and developed different equivalent-circuit descriptions for each of them.

Hasegawa et al. carried these concepts further in [2]. This work discussed three MIS regions of operation, each separated from the others by a transition region and described by its own distinct equivalent-circuit model.

In [3] Jäger focused on what he called the "slow wave" region of propagation of the MIS line. Jäger deviated significantly from the treatments of [1] and [2] by proposing an equivalent-circuit model in which the resistance of the substrate is connected in

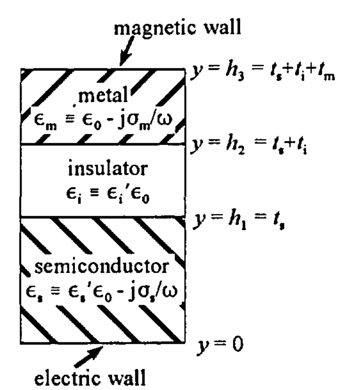

Fig. 1. The one-dimensional MIS transmission line.

parallel with the resistances of the metal and insulator, rather than in series with them.

These three investigations of the one-dimensional MIS lines have played a crucial role in shaping our understanding of the broader class of MIS transmission lines; almost all subsequent investigations of more complex MIS lines with fringing fields have focused on extensions of the basic circuit models they described.

This paper will report on a single, unified equivalent-circuit description for the dominant TM_0 mode of the one-dimensional MIS line. This paper will also investigate the common assumption that the TM_0 mode of the MIS line is always dominant and examine its properties when it becomes so lossy that it can no longer be considered dominant.

EXACT MODAL SOLUTIONS

It is customary to refer to the *n*th transverse-magnetic mode of a transmission line, where n refers to the order of the mode, as the TM_n mode. When the transmission line is lossless, n refers to the number of nulls in transverse magnetic field, and higher values of n correspond to higher spatial variation in the transverse fields. When the transmission line is lossy, the modes are ordered so that the transverse variation in the transverse fields increases with increasing n.

Reference [4] outlines a method of solving exactly for the propagation constant and fields of any TM_n mode of the one-dimensional transmission line of Fig. 1.

The usual definitions for the modal voltage v_0 and the modal current i_0 per unit width are

$$v_0 \equiv -\int_{y=0}^{h_3} E_y \, dy \qquad (1)$$

and

$$i_0 \equiv \oint H \cdot \mathrm{d}l = H_x|_{y=h_2}. \qquad (2)$$

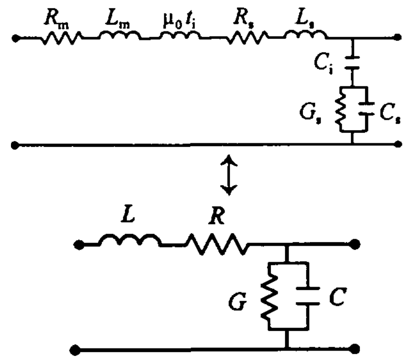

$$R + j\omega L \equiv (R_m + R_s) + j\omega\,(L_m + \mu_0 t_i + L_s)$$

$$G + j\omega C \equiv [\,(j\omega\, C_i)^{-1} + (G_s + j\omega\, C_s)^{-1}\,]^{-1}$$

Fig. 2. An equivalent-circuit model for the TM_0 mode of the MIS transmission line of Fig. 1. The formulas at the bottom of the figure can be used to transform between the model parameters and the line's standard circuit parameters R, L, G, and C plotted in Figs. 3-8. The inductance attributed to the insulating region in the model is $\mu_0 t_i$.

Here the modal voltage v_0 corresponds to the integral of the tangential electric field across the transmission line cross section from the electric wall at y=0 and the magnetic wall at $y=h_3$. The modal current i_0 corresponds to the current in the metal film, determined here by integrating the magnetic field around a path enclosing the metal. The modal power p_0 per unit width, equal to the integral of the Poynting vector over y, is

$$p_0 = -\int_{y=0}^{h_3} E_y \, H_x^* dy. \qquad (3)$$

In accordance with [5] and [6], the power-voltage definition of the characteristic impedance is $Z_0 \equiv |v_0|^2/p_0^*$ and the power-current definition of characteristic impedance is $Z_0 \equiv p_0/|i_0|^2$. We determine the inductance L, capacitance C, resistance R, and conductance G per unit length and width of the line from $R+j\omega L \equiv \gamma Z_0$ and $G+j\omega C \equiv \gamma/Z_0$.

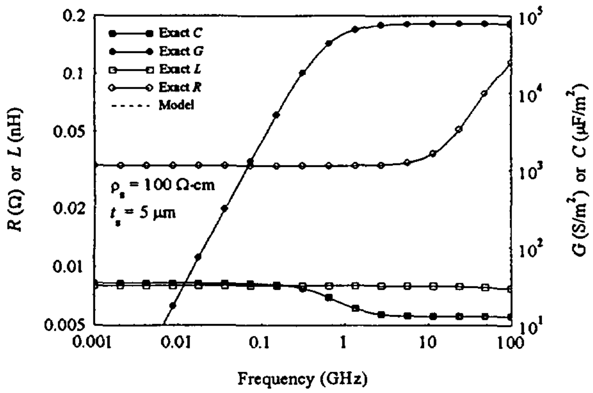

Fig. 3. Exact and modeled values of R, L, G, and C for the TM_0 mode of an MIS transmission line with $t_m = t_i =$ 1 μm, $\sigma_m = 3\times10^7$ S/m, $\epsilon_i' = 3.9$, $\epsilon_s' = 11.7$, $\rho_s = 100$ Ω·cm, and $t_s = 5$ μm. The model agrees so well with the exact results that the differences shown in the figure are indistinguishable. The exact values are calculated from the power-current definition of characteristic impedance.

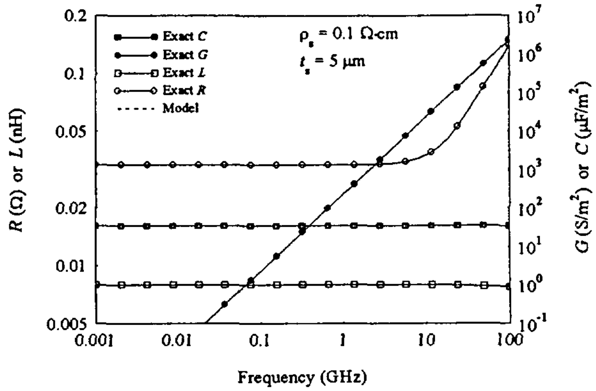

Fig. 4. Exact and modeled values of R, L, G, and C for the TM_0 mode of an MIS transmission line with $t_m = t_i =$ 1 μm, $\sigma_m = 3\times10^7$ S/m, $\epsilon_i' = 3.9$, $\epsilon_s' = 11.7$, $\rho_s = 0.1$ Ω·cm, and $t_s = 5$ μm. The model agrees so well with the exact results that the differences shown in the figure are indistinguishable. The exact values are calculated from the power-current definition of characteristic impedance.

MODEL

We will investigate a simple equivalent-circuit model for the TM_0 mode of the MIS line based on classic surface-impedance and parallel-plate-capacitor approximations. While this model cannot be found in the literature, it is really a compilation of models found in [1], [2], and [3].

Figure 2 shows the model elements and their relationships to the standard parameters R, L, G, and C. Define the complex dielectric constant ϵ_m of the metal to be $\epsilon_0 - j\sigma_m/\omega$, where ϵ_0 is the permittivity of free space, σ_m is the conductivity of the metal, and ω is the angular frequency, the dielectric constant ϵ_i of the insulator to be $\epsilon_i'\epsilon_0$, where ϵ_i' is the relative dielectric constant of the insulator, and the complex dielectric constant ϵ_s of the semiconductor to be $\epsilon_s'\epsilon_0 - j\sigma_s/\omega$, where ϵ_s' is its relative dielectric constant and σ_s is its conductivity. The obvious analogy of the MIS line with a parallel plate capacitor suggests setting $G_i + j\omega C_i$ and $G_s + j\omega C_s$ in the model of Fig. 2 to $j\omega\epsilon_i/t_i$ and $j\omega\epsilon_s/t_s$. Figures 3-8 compare the exact values of C and G for various substrate conductivities to those calculated from this model, which is marked with short dashed lines in the figures. The figures show that this model describes the TM_0 mode so well on highly resistive silicon substrates that the exact and model results are nearly indistinguishable, although Fig. 8 shows that the model overestimates G significantly at high frequencies on thick highly conductive substrates.

The classic surface-impedance formulation approximates R_m and L_m by the surface impedance of a plane wave impinging on the finite metal film backed by a magnetic wall, and R_s and L_s by the surface impedance of a plane wave impinging on the finite thickness semiconducting substrate backed by a perfectly conducting ground plane. The resulting expression for R_m and L_m in the model of Fig. 2 is

$$R_m + j\omega L_m \approx \frac{jk_{m1}}{\omega\epsilon_m}\,\frac{1}{\tan(k_{m1}t_m)} \qquad (4)$$

and for R_s and L_s is

$$R_s + j\omega L_s \approx \frac{jk_{s1}}{\omega\epsilon_s}\tan(k_{s1}t_s), \qquad (5)$$

where the $k_{\tau 1} \equiv \omega\sqrt{\mu_0\epsilon_\tau}$ [1].

Figures 3-8 compare the exact values of R and L (solid lines) to those calculated from this surface

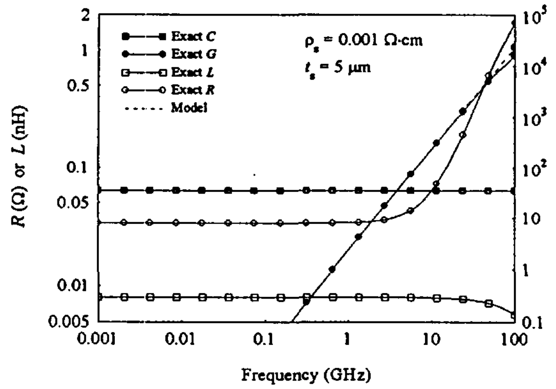

Fig. 5. Exact and modeled values of R, L, G, and C for the TM_0 mode of an MIS transmission line with $t_m = t_i =$ 1 μm, $\sigma_m = 3\times10^7$ S/m, $\epsilon_i' = 3.9$, $\epsilon_s' = 11.7$, $\rho_s = 0.001$ Ω·cm, and $t_s = 5$ μm. The model agrees so well with the exact results that the differences shown in the figure are nearly indistinguishable. The exact values are calculated from the power-current definition of characteristic impedance.

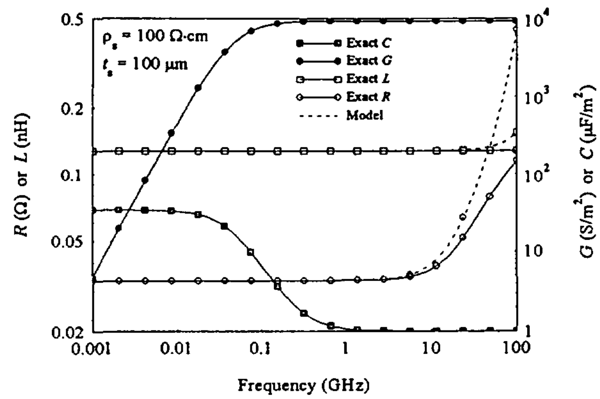

Fig. 6. Exact and modeled values of R, L, G, and C for the TM_0 mode of an MIS transmission line with $t_m = t_i =$ 1 μm, $\sigma_m = 3\times10^7$ S/m, $\epsilon_i' = 3.9$, $\epsilon_s' = 11.7$, $\rho_s = 100$ Ω·cm, and $t_s = 100$ μm. The exact values are calculated from the power-current definition of characteristic impedance.

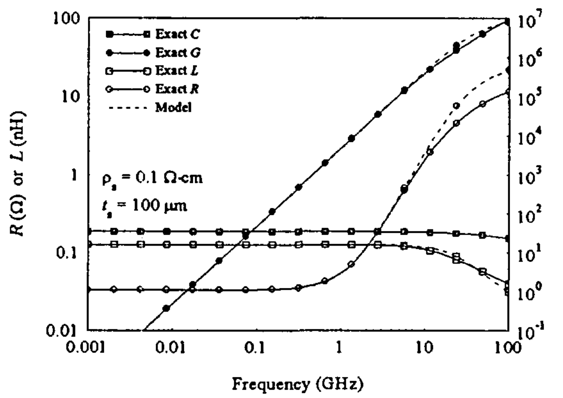

Fig. 7. Exact and modeled values of R, L, G, and C for the TM_0 mode of an MIS transmission line with $t_m = t_i =$ 1 μm, $\sigma_m = 3\times10^7$ S/m, $\epsilon_i' = 3.9$, $\epsilon_s' = 11.7$, $\rho_s = 0.1$ Ω·cm, and $t_s = 100$ μm. The exact values are calculated from the power-current definition of characteristic impedance.

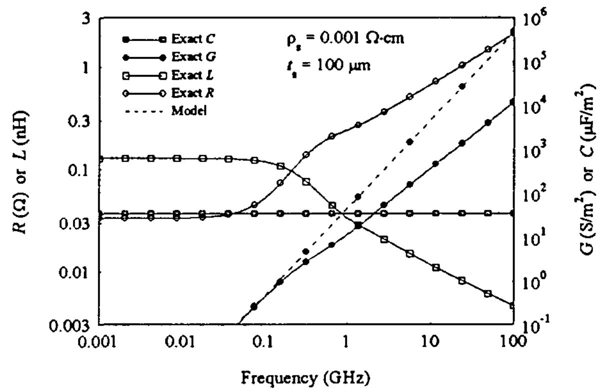

Fig. 8. Exact and modeled values of R, L, G, and C for the TM_0 mode of an MIS transmission line with $t_m = t_i =$ 1 μm, $\sigma_m = 3\times10^7$ S/m, $\epsilon_i' = 3.9$, $\epsilon_s' = 11.7$, $\rho_s = 0.001$ Ω·cm, and $t_s = 100$ μm. The exact values are calculated from the power-current definition of characteristic impedance.

impedance approximation, which are also marked with short dashed lines. Figures 3-5 show that this model so accurately predicts R and L on thin semiconductor substrates that the exact and modeled results are indistinguishable. However, Figs. 6-8 show that the model overestimates R and L significantly at high frequencies on thick highly resistive substrates. Thus, while the model always gives good results for thin substrates, at high frequencies and on thick substrates it overestimates G and C when the substrate conductivity is high and overestimates R and L when the substrate conductivity is low.

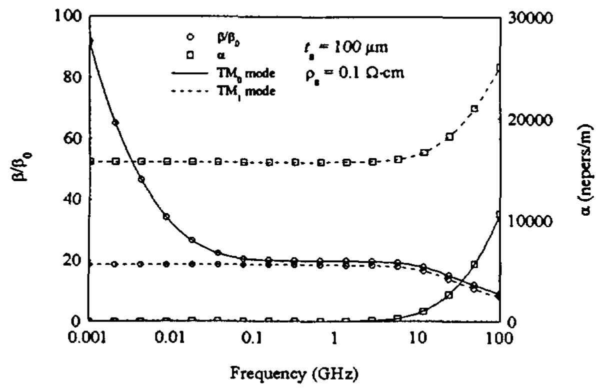

Fig. 9. The attenuation constant α and normalized phase constant β/β_0 of the TM_0 and TM_1 modes at $\rho_s = 0.1$ Ω·cm for an MIS transmission line with $t_m = t_i = 1$ μm, $\sigma_m = 3\times10^7$ S/m, $\epsilon_i' = 3.9$, $\epsilon_s' = 11.7$, and $t_s = 100$ μm. The quantities α and β are defined from $\gamma \equiv \alpha + j\beta$ and β_0 is the phase constant of a plane wave propagating in free space.

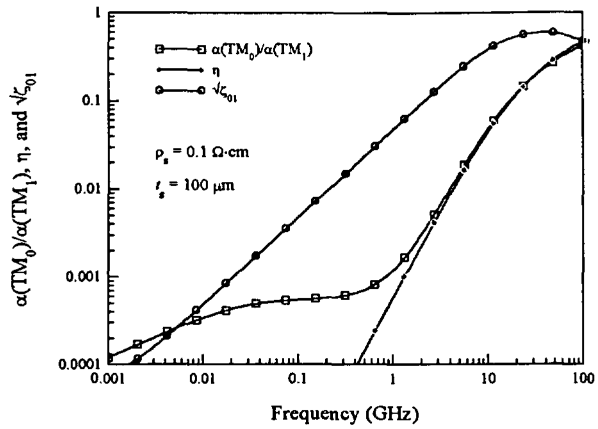

Fig. 10. The ratio of attenuation constants of the TM_0 and TM_1 modes, η, and ς_{01} at $\rho_s = 0.1$ Ω·cm for an MIS transmission line with $t_m = t_i = 1$ μm, $\sigma_m = 3\times10^7$ S/m, ϵ_i' = 3.9, $\epsilon_s' = 11.7$, and $t_s = 100$ μm.

HIGH LOSS REGION OF OPERATION

Although the exact method can be used to find the propagation constant and fields of any TM_n mode, up to this point we have examined only the TM_0 mode. When the substrate is thin the loss of the TM_0 mode is always small compared to those of the higher order modes of propagation, and it can be considered to be "dominant." That is to say, its loss is so low that all higher order modes created at a discontinuity in the line die away quickly enough to be ignored at small distances from the discontinuity. When the TM_0 mode is dominant it is the only mode that carries power between well separated sources, discontinuities, and receivers in the line. Figure 9 plots the attenuation constants α of the TM_0 and TM_1 modes as a function of frequency when $\rho_s = 0.1$ Ω·cm for a substrate thickness of t_s=100 μm. The figure shows that, at low frequencies, the attenuation of the TM_0 mode remains small compared to that of the TM_1 mode. At these frequencies the TM_0 is dominant, has fairly low attenuation, and is thus well suited for propagating electrical signals.

However, the attenuation constant of the TM_0 modes grows rapidly at high frequencies, making it poorly suited for propagating high frequency signals. Figure 10 shows that this high loss region is limited to high frequencies.

Figure 9 shows that in its high loss region of propagation, the attenuation constant of the TM_0 mode becomes comparable to that of the TM_1 mode. Here we can no longer say that the TM_0 mode is dominant and an accurate description of the line will require consideration of multiple modes of propagation, a considerable design complication. There are other design complications in this high loss region as well.

Figure 10 plots $\zeta_{01} \equiv |p_{01}p_{10}/p_{00}p_{11}|$, a measure of the significance of the modal cross powers [7], where

$$p_{nm} \equiv -\int_{y=0}^{h_3} E_{yn} H_{xm}^{*} dy \qquad (6)$$

and E_{yn} and H_{xn} are the fields of the TM_n mode. It shows that ζ_{01} becomes large when the propagation constants of the two modes become comparable. When ζ_{01} is large, the total power in the transmission line can no longer be calculated as a sum of the powers carried individually by the TM_0 and TM_1 modes [8]. This emphasizes the complexity and multimodal character of the transmission line in its high loss region of operation.

Figure 10 also plots $\eta \equiv |v_0 i_0^* - p_0| / |p_0|$, a measure of the fidelity with which the power carried by the TM_0 mode is determined by the product $v_0\, i_0^*$ of its modal voltage and the conjugate of its modal current. The figure shows that the usual relationship between the conventionally defined modal voltage and current and the actual power carried in the line fails in the high loss region.

MIS lines with high loss regions of operation may be used to propagate low-frequency signals over moderate distances and high frequency signals over very short distances. However, the preceding discussion paints a complex picture of the electromagnetic behavior of the MIS line there. Accurate high-frequency circuit design in this high loss region will require accounting for the multimodal character of the transmission line, the high modal cross powers, and the unconventional relationships between the modal voltage, current, and power.

CONCLUSION

This paper presented a closed-form model for the equivalent-circuit parameters of the TM_0 mode of the one-dimensional MIS transmission line. In contrast to previous treatments only a single set of expressions and model topology are required to describe the line over its entire range of operating conditions. This simplification creates a clear physical picture of the MIS line, in which the impedances and admittances of each layer may be calculated independently and then added together in a simple and intuitive way to predict overall transmission line behavior. In this picture the series impedance of each layer is determined by its surface impedance and its admittance by a parallel plate capacitance model.

This paper has also shown that the MIS line has a high loss region of operation in which its electrical behavior becomes complicated and multimodal in nature. It explored the properties of the TM_0 mode in this high loss region of operation, showing that the conventional relationships between its modal voltage, current, and power do not hold there, and that the total power in the line is no longer a simple sum of the powers carried by each mode of propagation individually. From this last observation, we can conclude that accurate treatments of MIS lines in this high loss region will require consideration not only of multiple modes of operation, but also of the modal cross powers, as is done in [8].

This paper has not addressed the applicability of the model to microstrip lines, nor has it attempted to develop a model that accounts for field variations in the line. Reference [9] will address these issues in detail.

ACKNOWLEDGMENTS

I thank Uwe Arz and Donald DeGroot for sharing with me their many useful insights concerning the physics of the MIS transmission line.

REFERENCES

[1] H. Guckel, P. A. Brennan, and I. Palócz, "A parallel-plate waveguide approach to microminiaturized, planar transmission lines for integrated circuits," *IEEE Trans. Microwave Theory and Tech.*, vol. MTT-15, no. 8, pp. 468-476, Aug. 1967.

[2] H. Hasegawa, M. Furukawa, and H. Yanai, "Properties of microstrip line on $SiSiO_2$ system," *IEEE Trans. Microwave Theory and Tech.*, vol. MTT-19, no. 11, pp. 869-881, Nov. 1971.

[3] D. Jäger, "Slow-wave propagation along variable Schottky-contact microstrip line," *IEEE Trans. Microwave Theory and Tech.*, vol. MTT-24, no. 9, pp. 566-573, Sept. 1976.

[4] R.E. Collins, *Field Theory of Guided Waves*. McGraw-Hill: New York, 1960.

[5] R. B. Marks and D. F. Williams, "A general waveguide theory," *J. Res. Natl. Inst. Stand. Technol.*, vol. 97, no. 5, pp. 533-562, Sept.-Oct., 1992.

[6] J. R. Brews, "Transmission line models for lossy waveguide interconnections in VLSI," *IEEE Trans. Electron Dev.*, vol. ED-33, no. 9, pp. 1356-1365, Sept. 1986.

[7] D. F. Williams and F. Olyslager, "Modal cross power in quasi-TEM transmission lines," *IEEE Microwave Guided Wave Lett.*, vol. 6., no. 11, pp. 413-415, Nov. 1996.

[8] D. F. Williams, L. A. Hayden, R. B. Marks "A complete multimode equivalent-circuit theory for electrical design," *J. Res. Natl. Inst. Stand. Technol.*, vol. 102, no. 4, July-Aug., 1997.

[9] D.F. Williams, "Metal-Insulator-Semiconductor Transmission Lines," to be submitted to *IEEE Trans. Microwave Theory and Tech.*